

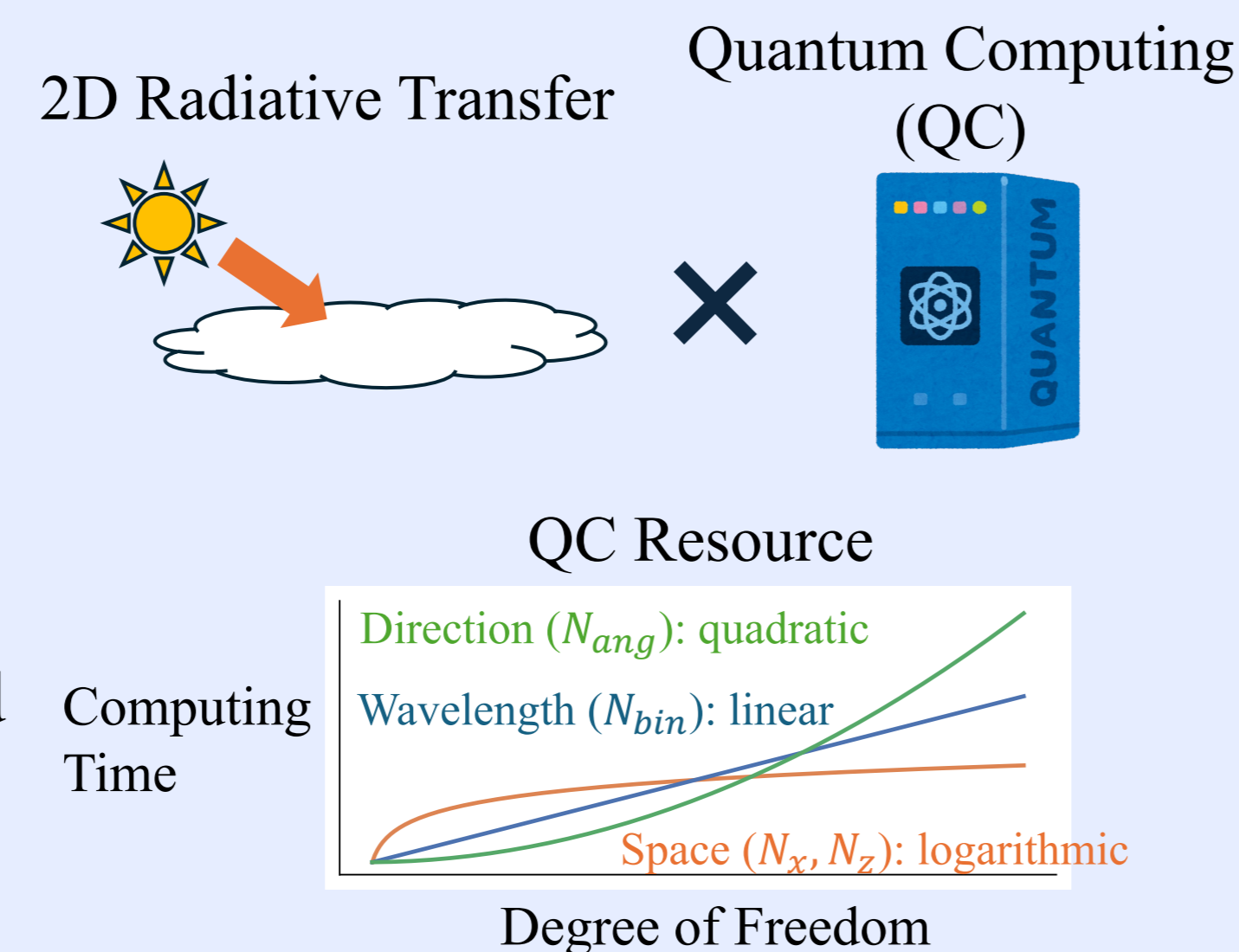


Key Points

Question: Can quantum computing reduce the cost of radiative transfer?

Answer: In this 2D DOM setting, the dependence on spatial resolution is low (good), while on angular resolution is comparatively high.

- The heating profile from our quantum algorithm matched that from a reference solution within a few percent.
- Readout remains a key challenge



Introduction

Quantum computing (QC) can be advantageous for some structured problems, but is constrained by unitarity and measurement overhead [1,2] (Fig. 1).

Radiative transfer is costly because it depends on space, direction, and wavelength. The discrete ordinate method (DOM) yields a large, sparse linear system.

Can QC accelerate steady-state DOM radiative transfer?

Goal: An initial assessment of the accuracy and resource scaling of a quantum algorithm for 2D radiative transfer.

New in this work: 1) explicit DOM block encoding, 2) condition-number and cost-scaling analysis

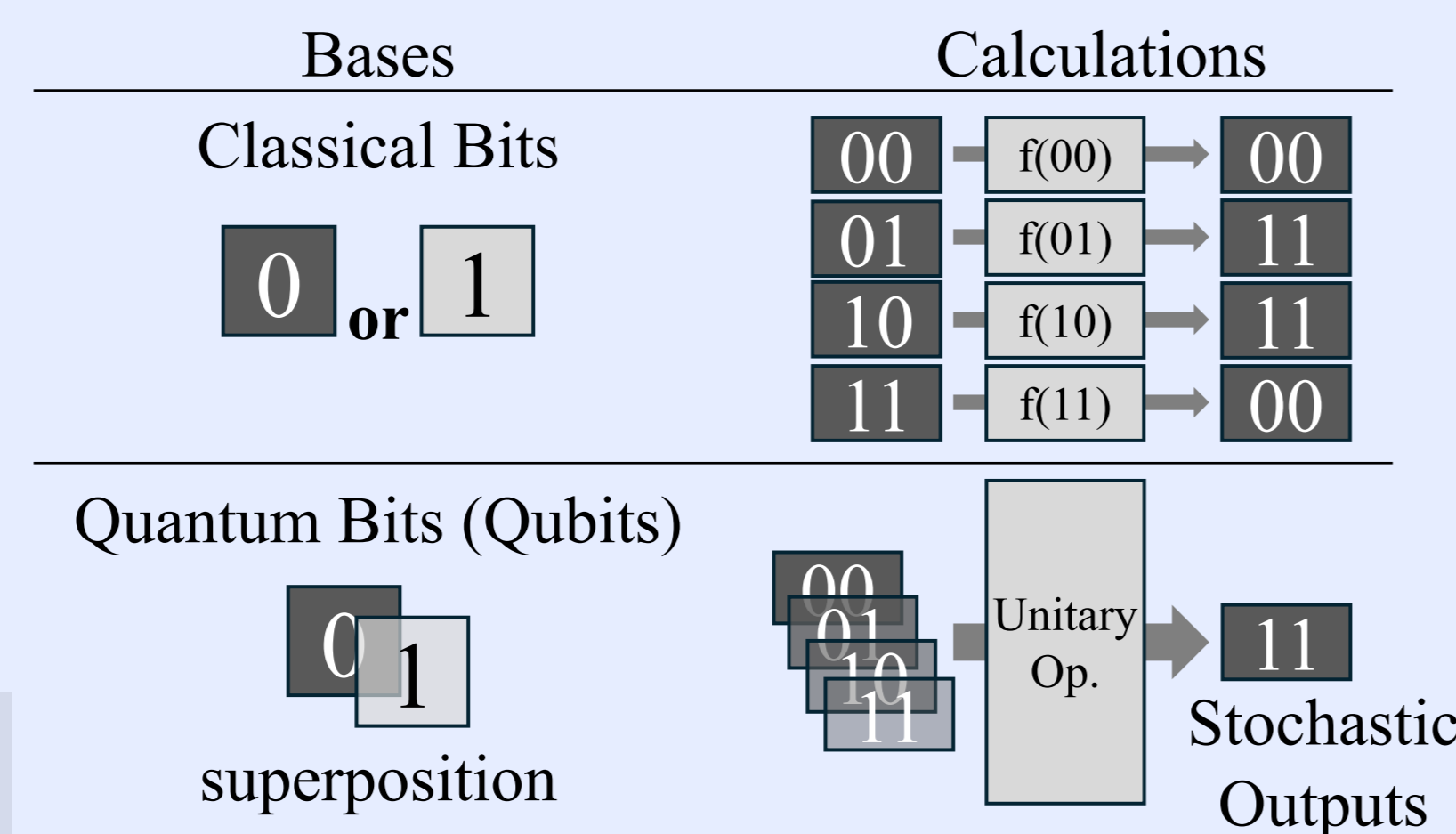


Fig. 1: Characteristics of classical computing (above) and quantum computing (below).

Methods

Formulation

Radiative Transfer Equation (RTE)

$$\boldsymbol{\Omega} \cdot \nabla l_{\lambda}(\mathbf{r}, \boldsymbol{\Omega}) = -\sigma_{t,\lambda}(\mathbf{r}) l_{\lambda}(\mathbf{r}, \boldsymbol{\Omega}) + j_{\lambda}(\mathbf{r}, \boldsymbol{\Omega}) + \sigma_{s,\lambda}(\mathbf{r}) \int P_{\lambda}(\boldsymbol{\Omega}, \boldsymbol{\Omega}') l_{\lambda}(\mathbf{r}, \boldsymbol{\Omega}') d\boldsymbol{\Omega}'$$

Streaming	Extinction	Thermal/source emission	Scattering from other directions
l_{λ} : radiance at wavelength λ , \mathbf{r} : spatial coordinate, $\boldsymbol{\Omega}$: unit vector in the propagation direction, c : speed of light,	j_{λ} : thermal emission coefficient, $\sigma_{t,\lambda}$: extinction coefficient, $\sigma_{s,\lambda}$: scattering coefficient, $P_{\lambda}(\boldsymbol{\Omega}, \boldsymbol{\Omega}')$: scattering phase function from direction $\boldsymbol{\Omega}'$ to $\boldsymbol{\Omega}$		

Discretization (Discrete Ordinate Method; DOM [3])

2D grid in (x_i, z_k)

Discrete angles Ω_n

$$l_{\lambda}(\mathbf{r}, \boldsymbol{\Omega}) \rightarrow l_{\lambda,i,k,n}$$

- $i \in \{0, \dots, N_x - 1\}$: horizontal grid index
- $k \in \{0, \dots, N_z - 1\}$: vertical grid index
- $n \in \{0, \dots, N_{ang} - 1\}$: angular index
- $\lambda \in \{0, \dots, N_{bin} - 1\}$: wavelength index

$$\mathbf{K}\mathbf{l} = \mathbf{b}$$

- Sparse matrix
- System size: $N_x \times N_z \times N_{ang} \times N_{bin}$
- Block diagonal in wavelength
- Nearly block diagonal in space, except for streaming terms.

Problem Setting (Fig. 2)

- 2D cloudy atmosphere in $x - z$
- Top solar input
- Atmospheric scattering, absorption, and thermal emission
- Lambertian reflection at the bottom

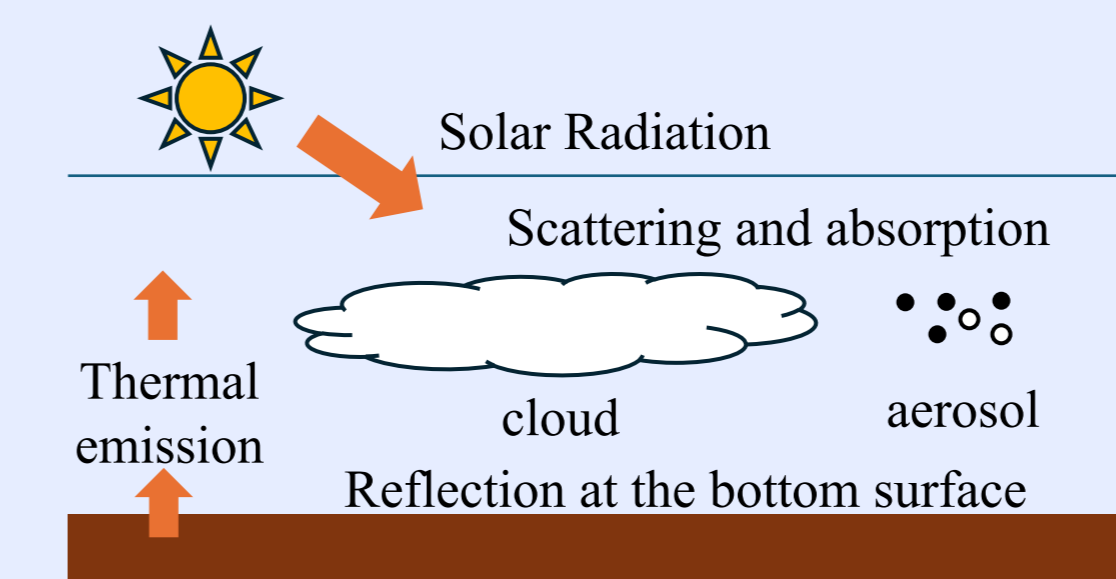


Fig. 2: Problem setting for RTE.

Quantum Algorithm

Quantum Solver Idea

Quantum Singular Value Transformation (QSVT [4], Fig. 4)

$$\mathbf{l} = \mathbf{K}^{-1}\mathbf{b} \approx \mathbf{V}f_d(\boldsymbol{\Sigma})\mathbf{U}^{\dagger}\mathbf{b}$$

$f_d(\boldsymbol{\Sigma})$: degree- d polynomial approximation of $\boldsymbol{\Sigma}^{-1}$ (Fig. 3)

Approximate the inverse action of \mathbf{K} by applying a degree- d polynomial approximation of $1/x$ to its singular values.

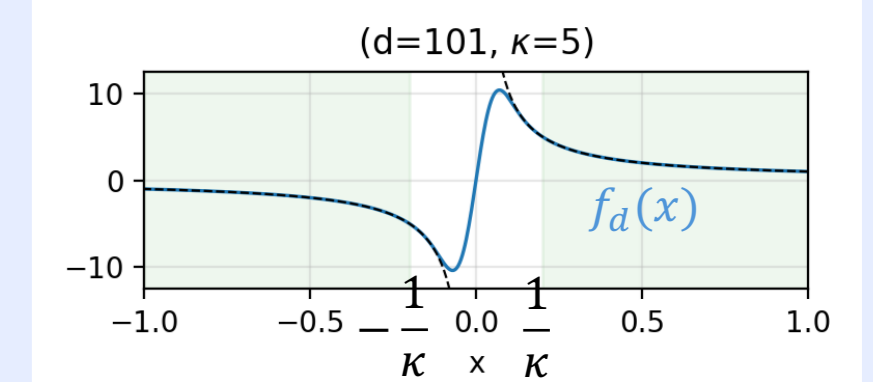


Fig. 3: Polynomial approx. of x^{-1} in $[-1, -1/\kappa] \cup [1/\kappa, 1]$

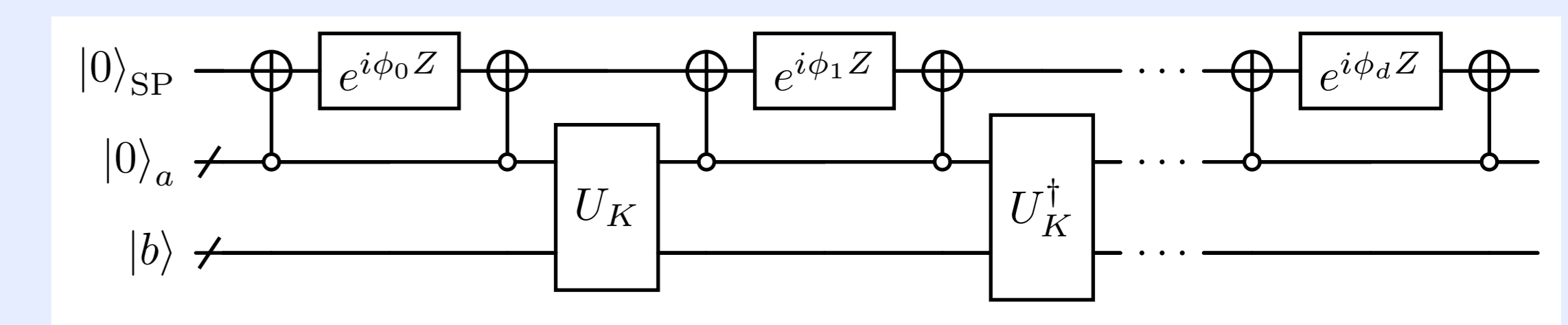


Fig. 4: Quantum circuit for solving a linear system using Quantum Singular Value Transformation (QSVT) [4]. Horizontal lines represent qubits, and boxes denote unitary operations on these qubits.

Block Encoding [4,5] of \mathbf{K} Polynomial Degree: d

$$U_K = \begin{pmatrix} \mathbf{K}/\alpha & * \\ * & * \end{pmatrix}$$

$$d = O(\kappa_{\text{eff}} \log(\kappa_{\text{eff}}/\epsilon)), \kappa_{\text{eff}} = \alpha/\sigma_{\text{min}}$$

- U_K : unitary encoding of \mathbf{K}/α
- α : normalization factor
- The structure of \mathbf{K} determines the cost of implementing U_K .
- κ_{eff} : effective condition number
- σ_{min} : smallest singular value of \mathbf{K}
- ϵ : tolerance error

The total cost is governed mainly by the polynomial degree (d) and the implementation cost of U_K .

Results

Simulation Results (Fig. 5)

- We run the new QSVT-based quantum circuit on a QC emulator on a classical computer and the results are compared with those by a direct solver.
- The heating rates derived from the radiance field agree between the two methods within a few percent.

Condition Number Analysis (Fig. 6)

- We analyzed the dependence of the effective condition number $\kappa_{\text{eff}} = \alpha/\sigma_{\text{min}}$ on the discretization parameters.
- κ_{eff} is nearly constant with respect to N_x and N_z , and scales linearly with N_{ang} .

Quantum Gate Counts of U_K (Fig. 7)

- We use the Toffoli count as a representative measure of circuit cost.
- The circuit cost scales logarithmically with N_x and N_z , and linearly with N_{ang} and N_{bin} .

Total QSVT Cost

- Approximately logarithmic in spatial resolution (N_x, N_z).
- Approximately quadratic in angular resolution N_{ang} (dominant cost).
- Approximately linear in wavelength bins N_{bin} .

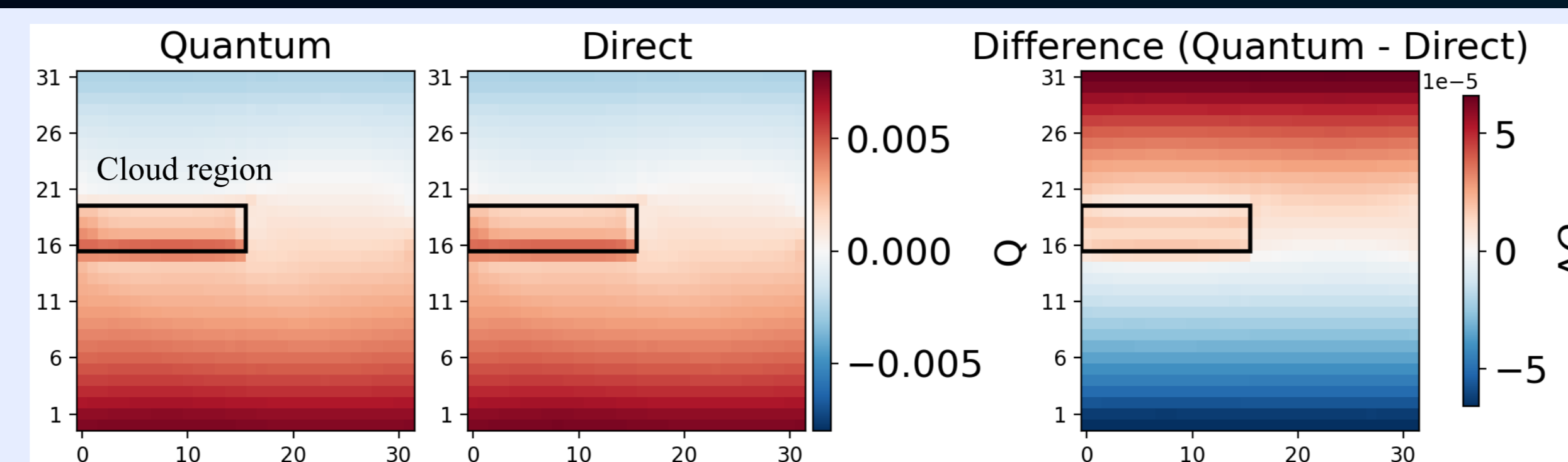


Fig. 5: Comparison of heating-rate profiles obtained from the QSVT-based simulation and a direct solver. For simplicity, the absorption and scattering coefficients are assumed to be uniform inside and outside the cloud. The QSVT parameters are set to $\kappa = 3000$ and $d = 30001$.

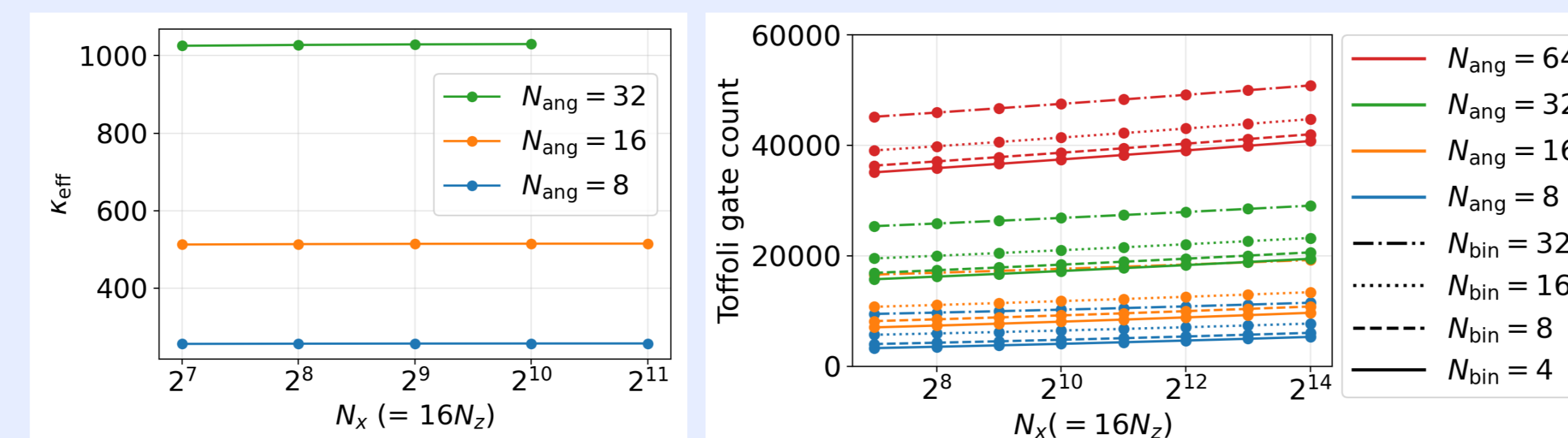


Fig. 6: Dependence of the effective condition number $\kappa_{\text{eff}} = \alpha/\sigma_{\text{min}}$ on the discretization parameters.

Fig. 7: Scaling of the Toffoli count with the discretization parameters after decomposing the full circuit, including multi-controlled gates. The Toffoli count is used here as a representative measure of circuit cost.

Discussion

Simplified Setting: The present analysis assumes uniform absorption and scattering coefficients both inside and outside the cloud, as well as a rectangular cloud geometry aligned with the spatial grid. This setting is simple, but the algorithm can be easily extended for more general media and geometries.

Readout Cost: The present resource analysis does not include the cost of extracting classical output from the final quantum state. Extracting the full radiance field can be expensive, so it may be practical to target selected observables, such as radiance at specific locations or summary quantities.

Future Work: Future work includes extensions to more realistic heterogeneous fields, alternative discretization methods, fully three-dimensional problems, and end-to-end resource analysis including readout cost.

References

- [1] Google Quantum AI and Collaborators. (2025). Observation of constructive interference at the edge of quantum ergodicity. *Nature*, 646(8086), 825–830. <https://doi.org/10.1038/s41586-025-09526-6>
- [2] Nielsen, M. A., & Chuang, I. L. (2010). *Quantum Computation and Quantum Information*. Cambridge University Press. <https://doi.org/10.1017/cbo9780511976667>
- [3] Stammes, K., Tsay, S. C., Wiscombe, W., & Jayaweera, K. (1988). Numerically stable algorithm for discrete-ordinate-method radiative transfer in multiple scattering and emitting layered media. *Applied Optics*, 27(12), 2502–2509. <https://doi.org/10.1364/AO.27.002502>
- [4] Gilyén, A., Su, Y., Low, G. H., & Wiebe, N. (2019, June 23). Quantum singular value transformation and beyond: exponential improvements for quantum matrix arithmetics. Proceedings of the 51st Annual ACM SIGACT Symposium on Theory of Computing. STOC '19: 51st Annual ACM SIGACT Symposium on the Theory of Computing, Phoenix AZ USA. <https://doi.org/10.1145/3313276.3316366>
- [5] Childs, A. M., Kothari, R., & Somma, R. D. (2017). Quantum algorithm for systems of linear equations with exponentially improved dependence on precision. *SIAM Journal on Computing*, 46(6), 1920–1950. <https://doi.org/10.1137/16m1087072>